

Copyright © 1990, by the author(s).
All rights reserved.

Permission to make digital or hard copies of all or part of this work for personal or classroom use is granted without fee provided that copies are not made or distributed for profit or commercial advantage and that copies bear this notice and the full citation on the first page. To copy otherwise, to republish, to post on servers or to redistribute to lists, requires prior specific permission.

**CALCULATION OF THE EMISSION
SPECTRUM OF DFB AND DBR LASERS**

by

Jean-Pierre Weber and Shyh Wang

Memorandum No. UCB/ERL M90/73

20 August 1990

**CALCULATION OF THE EMISSION
SPECTRUM OF DFB AND DBR LASERS**

by

Jean-Pierre Weber and Shyh Wang

Memorandum No. UCB/ERL M90/73

20 August 1990

ELECTRONICS RESEARCH LABORATORY

College of Engineering
University of California, Berkeley
94720

TITLE PAGE

**CALCULATION OF THE EMISSION
SPECTRUM OF DFB AND DBR LASERS**

by

Jean-Pierre Weber and Shyh Wang

Memorandum No. UCB/ERL M90/73

20 August 1990

ELECTRONICS RESEARCH LABORATORY

College of Engineering
University of California, Berkeley
94720

Calculation of the emission spectrum of DFB and DBR lasers

Jean-Pierre Weber
Shyh Wang

Department of Electrical Engineering and Computer Science
and Electronics Research Laboratory
University of California, Berkeley, CA 94720

ABSTRACT

We have developed a method based on transmission matrices that allows us to compute the emission spectrum of arbitrarily complicated semiconductor laser structures below and above threshold. These can include active and passive periodic or uniform sections. As examples, we compute the emission spectrum of a normal Distributed Feedback (DFB) laser, a DFB laser with a $\lambda/4$ phase shifter, and a surface-emitting Distributed Bragg Reflector (DBR) laser. We also discover some interesting features of the spontaneous emission in a periodic waveguide. These can be used to measure the coupling coefficient in a DFB laser with a $\lambda/4$ phase shifter.

August 20, 1990

Calculation of the emission spectrum of DFB and DBR lasers

Jean-Pierre Weber
Shyh Wang

Department of Electrical Engineering and Computer Science
and Electronics Research Laboratory
University of California, Berkeley, CA 94720

1. Introduction

Distributed Feedback (DFB) lasers are now widely used in long-distance communication systems because of the need for a single-mode operation and a high side-mode suppression ratio (35 to 40 dB). To obtain high suppression ratio, it is important to know how the various parameters of the laser are going to influence the emission spectrum. Distributed Bragg Reflector (DBR) laser structures are now widely studied to make frequency tunable lasers and are also used for vertical-cavity surface-emitting lasers. In both these cases, it would be desirable to be able to compute the emission spectrum.

In this paper, we will show how to compute the emission spectrum of these lasers without having to resort to numerical integration as was the case in the paper by Soda and Imai [1]. Because we use a model that considers the laser as an amplifier driven by spontaneous emission, our method is valid below, at and above threshold, as long as there is no spatial hole burning, since we will assume a uniform gain in each section of the devices we consider.

We will start by showing in section 2 how we can extend the usual transmission matrices theory to take into account sources that are in the structure we are analyzing. This allows us to apply this theory to lasers, which was not possible with the usual form of the transmission matrices technique. In section 3, we will give a brief summary of the theory of eigenmodes in a periodic structure, which is an alternative to coupled mode theory. The advantages of one theory over the other have been the subject of some discussions [2,3]. In this paper, we will show in section 4 that eigenmode theory has the advantage that it can be incorporated in a transmission matrices formalism (and it will also allow us to avoid numerical integrations when we compute the spectrum of a laser). In section 5, we compute the coupling of the spontaneous emission to

the eigenmodes. This then allows us to find how to compute the emission spectrum of a DFB laser in section 6 and show the result on an example in section 7. We will then show (in section 8) how to extend the method to compute the spectrum of an arbitrary structure and we will illustrate it with a DFB laser with a $\lambda/4$ phase shifter (in section 9). In section 10, we will briefly discuss some features of the emission spectrum of a $\lambda/4$ DFB laser that show the effect of the periodicity of the waveguide on the spontaneous emission. Finally, in section 11, we will extend the previous results to DBR lasers and take as an example a surface-emitting DBR laser.

2. Transmission matrices with sources

Usual transmission matrices (such as in Yariv and Yeh [4]), relate (see Fig. 1) the amplitudes of the waves going in and out of the structure at one end (A_1, B_1), at position z_1 , to the ones at the other end (A_2, B_2), at position z_2 . This can then be written as:

$$\begin{bmatrix} A_2 \\ B_2 \end{bmatrix} = T \begin{bmatrix} A_1 \\ B_1 \end{bmatrix} \quad (1)$$

where T is in general a 2×2 complex matrix and is a function of wavelength. The matrix T is always unimodular (i.e., its determinant is one).

Now, let us see how we can introduce a source at a position z_3 between z_1 and z_2 . We can always decompose (1) into two equations, one for the transmission from z_1 to z_3 (with a matrix R) and one for the transmission from z_3 to z_2 (with a matrix L). This gives us:

$$\begin{bmatrix} A_2 \\ B_2 \end{bmatrix} = L \begin{bmatrix} A_3 \\ B_3 \end{bmatrix} \quad \text{and} \quad \begin{bmatrix} A_3 \\ B_3 \end{bmatrix} = R \begin{bmatrix} A_1 \\ B_1 \end{bmatrix} \quad (2)$$

where $L R = T$ and A_3 and B_3 are the amplitudes of two power orthogonal modes at z_3 (not necessarily the same modes as at z_1 or z_2). Now, if we have a source at z_3 , this source would add to the amplitudes of the modes at that position, so that the first equation in (2) becomes:

$$\begin{bmatrix} A_2 \\ B_2 \end{bmatrix} = L \begin{bmatrix} A_3 - S_A \\ B_3 + S_B \end{bmatrix} \quad (3)$$

where S_A and S_B are the amplitudes added to the A and B modes, respectively. The minus sign in front of S_A is necessary because of the opposite direction of propagation of the A and B

modes. Notice that this is perfectly general since L and R can represent any arbitrarily complicated structure.

This method is correct and allows us to get all the results derived below, but there is a much more elegant way to express the same result. This is by using 3×3 matrices, in the following form:

$$\begin{bmatrix} A_2 \\ B_2 \\ 1 \end{bmatrix} = \begin{bmatrix} L_{11} & L_{12} & 0 \\ L_{21} & L_{22} & 0 \\ 0 & 0 & 1 \end{bmatrix} \begin{bmatrix} 1 & 0 & -S_A \\ 0 & 1 & S_B \\ 0 & 0 & 1 \end{bmatrix} \begin{bmatrix} R_{11} & R_{12} & 0 \\ R_{21} & R_{22} & 0 \\ 0 & 0 & 1 \end{bmatrix} \begin{bmatrix} A_1 \\ B_1 \\ 1 \end{bmatrix} \quad (4)$$

where the L_{ij} and R_{ij} are the elements of the L and R matrices defined above in (2). We can see that this gives the same result as (3), but with the advantage that we do not have to introduce any amplitudes for intermediate points. Also, this generalizes immediately to any number of sources at any position. But we should be careful here because this formulation assumes that all the sources are coherent. If they are not, we can still use this method for each source separately and then combine the powers.

Now, by using either (2)-(3) or (4), we can relate the output field to the sources in the case when there is no light injected into the structure (i.e., $B_1 = A_2 = 0$). Remembering that $L R = T$, we can then solve for A_1 and B_2 , which gives us:

$$\begin{aligned} A_1 &= \frac{1}{T_{11}} \left[L_{11} S_A - L_{12} S_B \right] \\ B_2 &= \frac{1}{T_{11}} \left[(T_{21} L_{11} - T_{11} L_{21}) S_A + (T_{11} L_{22} - T_{21} L_{12}) S_B \right] \end{aligned} \quad (5)$$

As an example of this technique, let us take a Fabry-Perot type cavity (Fig. 2). The total (3×3) transmission matrix T_{FP} for the cavity with a source can be obtained as the product of five matrices: T_1 , the matrix for transition between free space and the cavity modes at z_1 ; P_1 , the propagation matrix from z_1 to z_3 ; S , the source matrix at z_3 ; P_2 , the propagation matrix from z_3 to z_2 ; and T_2 , the transition matrix from cavity to free space modes. Thus:

$$\begin{aligned} T_{FP} &= T_2 P_2 S P_1 T_1 = L S R \\ \text{with } L &= T_2 P_2 \quad \text{and } R = P_1 T_1 \end{aligned} \quad (6)$$

(We will not distinguish between the 2×2 and 3×3 L and R matrices in the notation, since the

3×3 is trivially obtained from the 2×2 by adding a one on the diagonal and zeroes elsewhere. The distinction will be clear from the context.)

The 2×2 matrices are, in this case:

$$T_1 = \begin{bmatrix} \frac{1}{T_1} & -\frac{R_2}{T_1} \\ \frac{R_1}{T_1} & \frac{N_1}{T_1} \end{bmatrix} \quad P_1 = \begin{bmatrix} e^{j\beta(L-z_3)} & 0 \\ 0 & e^{-j\beta(L-z_3)} \end{bmatrix}$$

$$T_2 = \begin{bmatrix} \frac{1}{T_3} & -\frac{R_4}{T_3} \\ \frac{R_3}{T_3} & \frac{N_2}{T_3} \end{bmatrix} \quad P_2 = \begin{bmatrix} e^{j\beta z_3} & 0 \\ 0 & e^{-j\beta z_3} \end{bmatrix} \quad (7)$$

where the R_i and T_i are the reflection and transmission coefficients of the mirrors defined in Fig. 2 and

$$N_1 = T_1 T_2 - R_1 R_2$$

$$N_2 = T_3 T_4 - R_3 R_4 \quad (8)$$

Using this with (5) and (6), we get then:

$$A_1 = T_1 \frac{e^{-j\beta(L-z_3)} S_A + R_4 e^{-j\beta(L+z_3)} S_B}{1 - R_1 R_4 e^{-j2\beta L}}$$

$$B_2 = T_4 \frac{R_1 e^{-j\beta(2L-z_3)} S_A + e^{-j\beta z_3} S_B}{1 - R_1 R_4 e^{-j2\beta L}} \quad (9)$$

We can easily see that this is the same result as the one obtained by summing the multiple reflections. The advantage of this method is that it works also for much more complex structures. And, as we will see below, it can also be used for Distributed FeedBack (DFB) and Distributed Bragg Reflector (DBR) lasers.

3. Eigenmode theory summary

There are two ways to use transmission matrices in the case of a periodic structure. One is to use a matrix for each period and multiply them all. The other method is to treat, for example, a normal DFB laser as the Fabry-Perot we saw in the previous section, but with the plane wave modes inside the cavity replaced by the eigenmodes of the periodic structure and the corresponding modifications of the reflection and transmission coefficients and the propagation factors. We will use this second method here, but first let us look at a quick summary of some results of eigenmode theory that we will need (their derivation can be found in [5] and [6]).

If we have a one-dimensional even periodic structure of period Λ , the solution of the wave equation around the Bragg wavelength is of the Floquet-Bloch type and can be written as:

$$\begin{aligned} E(z, \lambda) &= A_0 [1 + s(\lambda) \exp(j2K_B z)] e^{\Gamma z} + B_0 [1 + s(\lambda) \exp(-j2K_B z)] e^{-\Gamma z} \\ &= A_0 [1 + s_f] e^{\Gamma z} + B_0 [1 + s_b] e^{-\Gamma z} \end{aligned} \quad (10)$$

where $K_B = p\pi/\Lambda$ (p is the order of the Bragg reflection), and A_0 and B_0 are the amplitudes of a forward and backward propagating mode, respectively. Notice that the origin ($z = 0$) must be at a point of even symmetry. The other coefficients are defined by:

$$\delta = K_B - \bar{\beta}(\lambda) \quad (11.a)$$

$$(G + j\delta_{eff})^2 = (g + j\delta)^2 + \kappa^2 \quad (11.b)$$

$$\Gamma = G + j\delta_{eff} - jK_B \quad (11.c)$$

$$s = \frac{j\kappa}{G + g + j(\delta + \delta_{eff})} \quad (11.d)$$

$$\lambda_0 = 2n_{eff} \Lambda/p \quad (11.e)$$

where g and $\bar{\beta}(\lambda)$ are the average amplitude gain and propagation constant in the periodic structure, and κ is the coupling constant ($= \beta_p$, the coefficient of $\exp(jp2\pi/\Lambda z)$ in the Fourier expansion of $\beta(z)$). Equation (11.b) is the dispersion relation of the periodic structure. If only the index of refraction is periodic, κ is real and, in the stop-band ($|\delta| < \kappa$), G is <0 if $g \leq 0$ and G is >0 if $g > 0$. Equation (11.e) expresses the Bragg condition and gives the Bragg wavelength λ_0 as a function of the effective refractive index (n_{eff}) and of the period Λ .

If the periodic structure does not have even symmetry and if the gain exhibits also some periodicity, things get more complicated. These effects are discussed at some length in [6]. It can also be shown that the choice of the root in (11.b) is arbitrary and does not change any measurable result (see [6]), and as a consequence, the designations forward and backward mode are also arbitrary and used only as means to distinguish the two modes. Both the modes carry power in both directions. We can usually choose the root of (11.b) such that the “forward” mode has a net power flow in the forward direction (take $|s| < 1$), but that is not necessary (see [6]).

We can then find a propagation factor D_f that relates the amplitude of the forward wave at a position z_1 to the amplitude at z_2 ($z_2 < z_1$). We can find a similar propagation factor D_b for the backward wave.

$$E_f(z_1) = D_{f,21} E_f(z_2) = \frac{1 + s \exp(j2K_B z_1)}{1 + s \exp(j2K_B z_2)} \exp(\Gamma L) E_f(z_2) \quad (12)$$

$$E_b(z_2) = D_{b,12} E_b(z_1) = \frac{1 + s \exp(-j2K_B z_2)}{1 + s \exp(-j2K_B z_1)} \exp(\Gamma L) E_b(z_1)$$

where $L = z_1 - z_2$. From the continuity of the tangential electric and magnetic fields, we can compute the reflection and transmission coefficient between a uniform and a periodic region. Appendix A gives these coefficients (which are derived in [5] and [6]).

4. Simple DFB laser

We can now consider a simple DFB laser, which has exactly the same structure as the Fabry-Perot laser in Fig. 2, except that the cavity is filled with a medium that is periodic in the z direction instead of being uniform. To do a transmission matrices analysis of this DFB laser, we need the same matrices as in (6)-(7). The matrices T_1 and T_2 are exactly the same as in (7), except that the R_i 's and T_i 's are given by Appendix A. The propagation matrices P_1 and P_2 can easily be found to be:

$$P_1 = \begin{bmatrix} \frac{1}{D_{f,31}} & 0 \\ 0 & D_{b,13} \end{bmatrix} \quad P_2 = \begin{bmatrix} \frac{1}{D_{f,23}} & 0 \\ 0 & D_{b,32} \end{bmatrix} \quad (13)$$

Then, by the same method as for the Fabry-Perot [i.e., by using (5)], we get:

$$A_1 = \frac{T_1}{1 - R_1 R_4 D_{f,21} D_{b,12}} \left[D_{f,31} S_A + D_{f,21} R_4 D_{b,32} S_B \right] \quad (14)$$

$$B_2 = \frac{T_4}{1 - R_1 R_4 D_{f,21} D_{b,12}} \left[D_{b,12} R_1 D_{f,31} S_A + D_{b,32} S_B \right]$$

where we used the fact [easily obtained from (12)] that:

$$\begin{aligned} D_{f,21} &= D_{f,23} D_{f,31} \\ D_{b,12} &= D_{b,13} D_{b,32} \end{aligned} \quad (15)$$

Now, one has to be careful about the meaning of S_A and S_B in this formula. They are the amplitude of the eigenmode of the periodic medium due to a source at position z_3 . This means that we have to compute the coupling coefficient between the source and the eigenmodes before we can compute the emission spectrum. This is what we are going to do in the next section. When that is known, we will use the result to obtain a relation between the power emitted by the source and the output power (as a function of wavelength). Then we will sum over the source position (i.e., integrate over z_3), which we will be able to do analytically.

To conclude this section, let us notice that there are several other ways to obtain the result (14). One of them is to sum the geometric series obtained by adding all the possible reflections, as one would do with a normal Fabry-Perot laser. Another one is to add eigenmode amplitudes in the cavity as unknowns and obtain a system of equations relating these to the sources and the output fields. This system can then be solved and gives (14) again. The transmission matrices method is used here because its generalization is more straightforward than the other methods.

5. Extension of Petermann's method for spontaneous emission coupling

In this section, we will compute the coupling between a source in a periodic waveguide and the two longitudinal eigenmodes corresponding to the fundamental transverse mode. The method we use is derived from the method of Petermann [7], but we extend it to take into account the periodicity of the waveguide. In this paper, we will treat only the simple case when the periodicity has even symmetry, but the theory can easily be extended to any shape of grating (see [6]). The wave equation for the waveguide without sources is of the form:

$$\nabla^2 E_x + \omega^2 \mu_0 \epsilon(x, y, z) E_x = 0 \quad (16)$$

with $\epsilon(x, y, z)$ periodic in the z direction. A good approximation to the solution can be written as:

$$E_x(x, y, z) = \sum_{i=0}^{i=+\infty} \left[D_i (1 + s_i e^{j2K_B z}) e^{\Gamma_i z} + D_{-i} (1 + s_i e^{-j2K_B z}) e^{-\Gamma_i z} \right] F_i(x, y) \quad (17)$$

where the $F_i(x, y)$ are the solutions of the transverse equation, the s_i are the corresponding s coefficients and the Γ_i are the corresponding propagation constants. We will not assume that the $F_i(x, y)$ are normalized to one, but we will assume that they can be taken as independent of z . They satisfy an orthogonality relation that we can write as:

$$\iint_{\mathbb{R}^2} F_i(x, y) F_j(x, y) dx dy = N^2 \delta_{i,j} \quad (18)$$

where $\delta_{i,j}$ is the Kronecker symbol and N is the (non-dimensional) normalization constant. Notice that the F_i 's have dimensions of $[m^{-1}]$ and the $D_{\pm i}$'s (as well as A_1 and B_2) have dimensions of Volts.

As the source in the waveguide, we will take a classical dipole oscillating at a frequency ω , situated at (x_p, y_p, z_p) and oriented parallel to the electric field (x direction). The wave equation with the source term is then:

$$\begin{aligned} \nabla^2 E_x + \omega^2 \mu_0 \epsilon(x, y, z) E_x &= j \omega \mu_0 J_x \\ &= j \omega \mu_0 (I l_d) \delta(x - x_p) \delta(y - y_p) \delta(z - z_p) \end{aligned} \quad (19)$$

where I and l_d are the current and dipole length of the source, respectively.

We will assume that the solution for $z > z_p$ can be written with the forward part of (17) (i.e., in D_{+i}) and the solution for $z < z_p$ can be written with the backward part (in D_{-i}). Expressing the field continuity at z_p gives us:

$$\sum_{i=0}^{+\infty} \left[D_{+i} (1 + s_i e^{j2K_B z_p}) e^{\Gamma_i z_p} - D_{-i} (1 + s_i e^{-j2K_B z_p}) e^{-\Gamma_i z_p} \right] F_i(x, y) = 0 \quad (20)$$

And if we integrate equation (19) from $z = z_p - 0$ to $z = z_p + 0$, we obtain:

$$\sum_{i=0}^{+\infty} \left[D_{+i} (\Gamma_i + (\Gamma_i + j2K_B) s_i e^{j2K_B z_p}) e^{\Gamma_i z_p} \right]$$

$$\begin{aligned}
 & +D_{-i} (\Gamma_i + (\Gamma_i + j2K_B) s_i e^{-j2K_B z_p}) e^{-\Gamma_i z_p} \Big] F_i(x, y) \\
 & = j \omega \mu_0 (I l_d) \delta(x - x_p) \delta(y - y_p)
 \end{aligned} \tag{21}$$

By using the orthogonality relation (18), we can now look at the fundamental mode, which is the one we are interested in. In the following, we will drop the i subscript, since we will always be working with the fundamental mode ($i = 0$). Thus, multiplying (20) and (21) by $F_0(x, y)$ and integrating over x and y gives us, respectively:

$$D_+ [1 + s e^{j2K_B z_p}] e^{\Gamma z_p} - D_- [1 + s e^{-j2K_B z_p}] e^{-\Gamma z_p} = 0 \tag{22}$$

and

$$\begin{aligned}
 & D_+ [\Gamma + (\Gamma + j2K_B) s e^{j2K_B z_p}] e^{\Gamma z_p} + D_- [\Gamma + (\Gamma + j2K_B) s e^{-j2K_B z_p}] e^{-\Gamma z_p} \\
 & = j \omega \mu_0 (I l_d) \frac{F_0(x_p, y_p)}{\iint F_0^2 dx dy}
 \end{aligned} \tag{23}$$

By solving the system of equations (22) and (23), we obtain the coefficients:

$$\begin{aligned}
 D_{\pm} & = \frac{1}{2} j \omega \mu_0 (I l_d) \frac{F_0(x_p, y_p)}{\iint F_0^2 dx dy} \\
 & \times \frac{(1 + s e^{\mp j2K_B z_p}) e^{\mp \Gamma z_p}}{\Gamma + (\Gamma + j2K_B) s^2 + 2s (\Gamma + jK_B) \cos(2K_B z_p)}
 \end{aligned} \tag{24}$$

Some signs in the result differ from the corresponding result in [6] because of an incorrect way (in [6]) of setting up the continuity equations (20) and (21). (However, this had no influence on the final result, the effect of the sign error disappears after integration). And if we take $z_p = z_3$, we see [from (17)] that the source terms in (14) are given by:

$$\begin{aligned}
 S_A & = D_+ (1 + s_{f3}) e^{\Gamma z_3} \\
 S_B & = D_- (1 + s_{b3}) e^{-\Gamma z_3}
 \end{aligned} \tag{25}$$

where s_{f3} means s_f calculated at $z = z_3$ and similarly for s_{b3} [s_f and s_b were defined in (10)].

6. Emission spectrum of a simple DFB laser

We are now nearly ready to compute the emission spectrum of a DFB laser. For simplicity, we will compute the output power through one facet only (the power through the other one is computed in the same way). So, we substitute (25) in the first equation of (14). By looking at Appendix A, (14) and (25), we notice that most factors of the form $(1 + s_f)$ and $(1 + s_b)$ actually cancel each other. So, if we redefine the propagation factors and reflection and transmission coefficients by omitting the factors inside square brackets in Appendix A, we can write:

$$\begin{aligned}
 A_1 = & \frac{1}{2} j \omega \mu_0 (I l_d) \frac{T_1}{1 - R_1 R_4 e^{2\Gamma(z_1 - z_2)}} \\
 & \times \frac{\left[e^{\Gamma(z_1 - z_3)} (1 + s_{b3}) + e^{\Gamma(z_1 + z_3 - 2z_2)} R_4 (1 + s_{f3}) \right]}{\Gamma + (\Gamma + j2K_B) s^2 + 2s (\Gamma + jK_B) \cos(2K_B z_3)} \\
 & \times \frac{F_0(x_3, y_3)}{\iint F_0^2 dx dy}
 \end{aligned} \tag{26}$$

Now, in this model we will assume that the wave of amplitude A_1 has the same transverse mode profile as the field in the cavity (a reasonable approximation). We can then find the total output power (for that facet) by integrating the Poynting vector over the cross-section:

$$P_{out} = \frac{k_0}{2 \omega \mu_0} |A_1|^2 \iint |F_0|^2 dx dy \tag{27}$$

where k_0 is the free space wavevector amplitude ($= 2\pi/\lambda$). And the total power radiated by the dipole is given [8] by:

$$P_{dip} = \sqrt{\frac{\mu_0}{\epsilon_0}} \frac{\omega^2 n}{12 \pi} \frac{(I l_d^2)}{c^2} \tag{28}$$

where n is the refractive index of the active region.

We can now find the ratio between the power radiated by the dipole and the output power (one facet) as:

$$\eta(x_3, y_3, z_3) = \frac{P_{out}}{P_{dip}} = \frac{3 \pi}{2 n} \frac{|T_1|^2}{|1 - R_1 R_4 e^{2\Gamma(z_1 - z_2)}|^2}$$

$$\begin{aligned} & \times \frac{|e^{\Gamma(z_1-z_3)}(1+s_{b3})+e^{\Gamma(z_1+z_3-2z_2)}R_4(1+s_{f3})|^2}{|\Gamma+(\Gamma+j2K_B)s^2+2s(\Gamma+jK_B)\cos(2K_Bz_3)|^2} \\ & \times \frac{|F_0(x_3,y_3)|^2}{|\iint F_0^2 dx dy|^2} \iint |F_0|^2 dx dy \end{aligned} \quad (29)$$

But in general, the dipoles are randomly oriented. If we average over the orientation, we will get a factor of 1/3. We also want to average over the distribution of dipoles in the transverse direction. We will assume that the distribution of dipoles $i_{dip}(x,y)$ (which is a density and has units $[\text{m}^{-3}]$) is constant. This is a good assumption if there is no longitudinal hole burning.

Let us define:

$$\frac{\Gamma_c}{d w_{eff}} = \frac{\iint |F_0(x,y)|^2 i_{dip}(x,y) dx dy}{\left[\iint i_{dip}(x,y) dx dy \right] \left[\iint |F_0(x,y)|^2 dx dy \right]} \quad (30)$$

where Γ_c is the energy confinement factor, d is the thickness of the waveguide and w_{eff} is an effective width for the waveguide. For a double heterostructure (i.e., an index-guided structure), $i_{dip}(x,y)$ is constant in the active region and zero elsewhere. Then w_{eff} is the real width, since Γ_c is defined by:

$$\Gamma_c = \frac{\iint_{\text{active region}} |F_0(x,y)|^2 dx dy}{\iint_{\mathbb{R}^2} |F_0(x,y)|^2 dx dy} \quad (31)$$

For a gain-guided structure, (30) defines an effective width w_{eff} . We are also going to use the K_P factor defined by Petermann [7]. It is a measure of the astigmatism of the wavefront in the guide:

$$K_P = \frac{\left[\iint |F_0(x,y)|^2 dx dy \right]^2}{|\iint F_0^2(x,y) dx dy|^2} \quad (32)$$

It is equal to one for index-guided structures (since the eigenmodes are then real).

We can now obtain the ratio between the output power and the power radiated by a dipole (at $z = z_3$), averaged over the dipole orientations and position in the transverse direction:

$$\begin{aligned}
 \bar{\eta}(z_3) &= \frac{1}{3} \frac{\iint \eta(x, y, z_3) i_{dip}(x, y) dx dy}{\iint i_{dip}(x, y) dx dy} \\
 &= \frac{\pi}{2n} \frac{\Gamma_c K_P}{w_{eff} d} \frac{|T_1|^2}{|1 - R_1 R_4 e^{2\Gamma L}|^2} \\
 &\quad \times \frac{|e^{\Gamma(z_1 - z_3)}(1 + s_{b3}) + e^{\Gamma(L + z_3 - z_2)} R_4 (1 + s_{f3})|^2}{|\Gamma + (\Gamma + j2K_B)s^2 + 2s(\Gamma + jK_B)\cos(2K_B z_3)|^2}
 \end{aligned} \tag{33}$$

where we used $L = z_1 - z_2$. And the next step is to average over the position in the cavity, i.e., z_3 . To do this averaging, we will proceed in two steps: first separate the slowly varying factors [$\exp(Gz)$ and $\exp(j\delta_{eff}z)$] from the rapidly varying factors [$\exp(jK_B z)$]. We notice then that the slowly varying factor change very little over one period Λ , so that we can average the rapidly varying factors over one period and then average the result over the length of the cavity. It has been shown (in [6]) that an exact analytic formula can be obtained for the average over one period by using the change of variables $u = \exp(j2K_B z)$, which gives an integral over the unit circle in the complex u plane. The result of the integral is then obtained by the residue method. But numerical examples show that we get the same result (with a relative error $< 10^{-3}$ for edge-emitting lasers and $< 2 \times 10^{-2}$ for surface-emitting lasers at all wavelengths of interest, in the worst case: no gain or loss), if we omit the cosine term in the denominator of the last factor in (33) before integrating over the period. We will use this approximation since the resulting expression is much simpler. Thus, the average over one period gives us:

$$\begin{aligned}
 \frac{1}{\Lambda} \int_0^\Lambda \bar{\eta} dz &= \frac{\pi}{2n} \frac{\Gamma_c K_P}{w_{eff} d} \frac{|T_1|^2}{|1 - R_1 R_4 e^{2\Gamma L}|^2} \frac{1}{|\Gamma + (\Gamma + j2K_B)s^2|^2} \\
 &\quad \times \left[(1 + |s|^2) \left[e^{2G(z_1 - z_3)} + |R_4|^2 e^{2G(L - z_2 + z_3)} \right] \right. \\
 &\quad \left. + 4 \operatorname{Re}(s) e^{2GL} \operatorname{Re} \left[R_4 e^{j2(K_B - \delta_{eff})z_2} e^{j2\delta_{eff}z_3} \right] \right]
 \end{aligned} \tag{34}$$

Now, by integrating the previous result from z_2 to z_1 and dividing by L , we get γ , the average of η over the whole cavity:

$$\gamma = \frac{\pi}{2n} \frac{\Gamma_c K_P}{w_{eff} d} \frac{|T_1|^2}{|1 - R_1 R_4 e^{2\Gamma L}|^2} \frac{1}{|\Gamma + (\Gamma + j2K_B)s^2|^2}$$

$$\times \left[(1 + |s|^2) \frac{(e^{2GL} - 1)}{2GL} (1 + |R_4|^2 e^{2GL}) \right. \\ \left. + 4 \operatorname{Re}(s) e^{2GL} \frac{\sin(\delta_{\text{eff}} L)}{\delta_{\text{eff}} L} \operatorname{Re} \left[R_4 e^{j\delta_{\text{eff}} L} e^{j2K_B z_2} \right] \right] \quad (35)$$

The dimensionless quantity γ that is given by (35) is a function of wavelength since s , Γ , G , and other variables are functions of wavelength. Assuming that the sources are uniformly distributed over the cavity (as is usually the case for spontaneous emission), we can now compute the total output power (through one facet) if we know the total power emitted by the sources. Explicitly, if $r_{sp}(\lambda)$ is the spontaneous emission rate spectral density per unit volume, the output power spectral density $P_{out}(\lambda)$ is given by:

$$P_{out}(\lambda) = \left[\frac{hc}{\lambda} \right] \left[r_{sp}(\lambda) d w_{\text{eff}} L \right] \gamma(\lambda) \quad (36)$$

where h is Planck's constant, c the speed of light and $d w_{\text{eff}} L$ is the total active volume. In edge-emitting lasers, one can usually assume that r_{sp} is about constant in the spectral range of interest or approximate it with a parabolic profile, but in surface-emitting devices, one has to use a more realistic model (as was done in [6]). If the spontaneous emission is constant in the spectral range of interest, $\gamma(\lambda)$ is then proportional to the emission spectrum we were looking for.

Notice that (35) also allows us to find the threshold condition. Indeed, we will be at threshold if γ becomes infinite, i.e., if a factor in the denominator becomes zero. It is easy to see that this means:

$$R_1 R_4 e^{2GL} = 1 \quad (37)$$

which is exactly the expression for a Fabry-Perot cavity, except that we have an effective gain G instead of the actual gain g . This is a complex equation for which the two unknowns are the amplitude gain and wavelength at threshold. It can also be transformed into the usual expression for the threshold of a DFB laser, using R_1 and R_4 from Appendix A (without the terms between square brackets) and (11).

7. Example of simple DFB laser

We will take as an example a quaternary DFB laser with a center wavelength of $1.528 \mu\text{m}$, $n_{\text{eff}} = 3.2336$ (which gives $\Lambda = 236.3 \text{ nm}$). The coupling coefficient κ will be 100 cm^{-1} . We will assume a length $L = 300 \mu\text{m}$ and that we have antireflection coating, so that the result becomes independent of z_2 [since in that case $R_4 \exp(2jK_B z_2) = s$ and $R_1 R_4 = s^2 \exp(2jK_B L)$] and all dependences are only on $L = z_1 - z_2$. In that case, by solving (37), we see that we have two degenerate modes, symmetrically located on each side of the Bragg wavelength of $1.528 \mu\text{m}$, at $\lambda = 1.5296 \mu\text{m}$ and $1.5264 \mu\text{m}$, with a threshold amplitude gain of 20.754 cm^{-1} (the slight height difference is due to numerical imprecisions). The next two modes are situated at $1.5254 \mu\text{m}$ and $1.5306 \mu\text{m}$, with a threshold 44.26 cm^{-1} . Figure 3 shows the emission spectrum calculated with (36), assuming no spectral dependence of the gain and the spontaneous emission rate. Three curves are shown, corresponding to three different values of the amplitude gain.

If the facets are not anti-reflection coated, the spectrum is going to be a function of the phase of the grating at the facets (i.e., a function of z_1 and z_2 and not only a function of L). As an illustration, Figure 4(a) shows the spectrum of the same laser, but with no coatings, with $z_2 = 0$ (the facet is at a point of even symmetry of the grating). The lowest threshold mode is then at $1.5262 \mu\text{m}$, with a threshold amplitude gain of 10.635 cm^{-1} . Figure 4(b) shows the spectrum of the same device, but with $z_2 = 100 \text{ nm}$. In that case, the main mode is at $1.5295 \mu\text{m}$, with a threshold amplitude gain of 8.896 cm^{-1} . This illustrates once again the problem of mode control for simple DFB lasers: with anti-reflection coating, there are two degenerate modes and without anti-reflection coating, the phase of the grating at the facet has to be controlled very accurately (within 25 nm), which is nearly impossible. This is why people are using more complicated structures such as DFB lasers with a $\lambda/4$ phase shifter, which we will see how to analyze in the next section.

8. General DFB structures

To compute the emission spectrum of a multisection DFB laser such as the DFB with a $\lambda/4$ phase shifter is basically very simple. The calculation for each section is exactly the same as for the simple DFB laser, except that T_1 and T_2 (the two transmission matrices at each end of the periodic section) are replaced with more complicated matrices accounting for the rest of the structure.

To make it easier to perform the summation over all the sources in the same periodic section, let us reformulate (4). Assume that there are n periodic sections in which there is spontaneous emission. We must use a different coordinate system in each section (since the origin has to be at a point of even symmetry). Each section will go from $z_2^{(i)}$ to $z_1^{(i)}$. For a source in section i at $z_3^{(i)}$, we can write:

$$\begin{bmatrix} A_2 \\ B_2 \\ 1 \end{bmatrix} = \begin{bmatrix} L_{11}^{(i)} & L_{12}^{(i)} & 0 \\ L_{21}^{(i)} & L_{22}^{(i)} & 0 \\ 0 & 0 & 1 \end{bmatrix} \begin{bmatrix} \frac{1}{D_{f,21}^{(i)}} & 0 & -\frac{S_A^{(i)}}{D_{f,23}^{(i)}} \\ 0 & D_{b,12}^{(i)} & D_{b,32}^{(i)} S_B^{(i)} \\ 0 & 0 & 1 \end{bmatrix} \begin{bmatrix} R_{11}^{(i)} & R_{12}^{(i)} & 0 \\ R_{21}^{(i)} & R_{22}^{(i)} & 0 \\ 0 & 0 & 1 \end{bmatrix} \begin{bmatrix} A_1 \\ B_1 \\ 1 \end{bmatrix} \quad (38)$$

where $L^{(i)}$ and $R^{(i)}$ are now the transmission matrices for everything to the left and the right of section i , respectively (but without the periodic section itself). This allows us to rewrite (5) as:

$$A_1 = \frac{1}{T_{11}} \left[L_{11}^{(i)} \frac{S_A^{(i)}}{D_{f,23}^{(i)}} - L_{12}^{(i)} D_{b,32}^{(i)} S_B^{(i)} \right] \quad (39)$$

$$B_2 = \frac{1}{T_{11}} \left[(T_{21} L_{11}^{(i)} - T_{11} L_{21}^{(i)}) \frac{S_A^{(i)}}{D_{f,23}^{(i)}} + (T_{11} L_{22}^{(i)} - T_{21} L_{12}^{(i)}) D_{b,32}^{(i)} S_B^{(i)} \right]$$

where T is independent of i , since it represents the whole structure.

Now, by going through the same sequence of steps as in section 4, we will be able to obtain $\gamma^{(i)}(\lambda)$, the power coupling factor for section (i). And the total output power spectral density will then be given by:

$$P_{out}(\lambda) = \sum_{i=1}^n \gamma^{(i)}(\lambda) P_{sp}^{(i)}(\lambda) \quad (40)$$

where $P_{sp}^{(i)}(\lambda)$ is the total spontaneous emission spectral power density for section i .

To compute $\gamma^{(i)}$, we use the same assumptions as in section 4: all the $(1+s_f)$ and $(1+s_b)$ factors (the ones between square brackets in Appendix A) have already been cancelled, the averaging over $z_3^{(i)}$ is done first by averaging over a period, then over the section's length $L^{(i)}$.

We get then:

$$\begin{aligned} \gamma^{(i)}(\lambda) = & \frac{\pi}{2n^{(i)}} \frac{\Gamma_c^{(i)} K_P^{(i)}}{w_{eff}^{(i)} d^{(i)}} \frac{1}{|T_{11}|^2} \frac{1}{|\Gamma^{(i)} + (\Gamma^{(i)} + j2K_B^{(i)})(s^{(i)})^2|^2} \\ & \times \left[\frac{(1+|s^{(i)}|^2)}{2G^{(i)}L^{(i)}} \left[|L_{11}^{(i)}|^2 (1 - e^{-2G^{(i)}L^{(i)}}) + |L_{12}^{(i)}|^2 (e^{2G^{(i)}L^{(i)}} - 1) \right] \right. \\ & \left. - 4 \operatorname{Re}(s^{(i)}) \frac{\sin(\delta_{eff}^{(i)} L^{(i)})}{\delta_{eff}^{(i)} L^{(i)}} \operatorname{Re} \left[(L_{11}^{(i)})^* L_{12}^{(i)} e^{j\delta_{eff}^{(i)} L^{(i)}} e^{j2K_B^{(i)} z_2^{(i)}} \right] \right] \end{aligned}$$

where the asterisk indicates the complex conjugate.

And we can readily see that the threshold condition for such a structure is given by:

$$T_{11} = 0 \quad (42)$$

which gives (37) for the simple DFB laser.

9. Quarter-wavelength phase-shifted DFB

As a simple example of a more complicated DFB structure, let us look at a DFB laser with a $\lambda/4$ phase-shifter in the middle. We will assume that the two sections of grating are identical and have the same gain, so that κ , s and Γ are the same. Figure 5 shows the structure and defines the reflection and transmission coefficients (which are given in Appendix B). Notice that R_5 , R_6 , T_5 and T_6 are for the whole phase shifter section (see Appendix B and [6]). The phase shifter has a length $L_P = \lambda/4n_{eff}$.

For simplicity, we will neglect the spontaneous emission from the phase-shifter region, since it is very small. (If we want to take that into account, we can use the DBR method explained in a following section and add the contribution to the spectrum calculated here.) Figure 5 shows the coordinate system in each section. We will choose the origins on the edges of the

active region, i.e., $z_1^{(1)} = 0$ and $z_2^{(2)} = 0$. (This choice is correct if the grating is made the way it is shown in Figure 5.)

For the spectrum calculation, we do not need all the elements of the transmission matrices.

We need only:

$$T_{11} = \frac{D}{T_1 T_3 T_5 D_f^{(1)} D_f^{(2)}}$$

$$L_{11}^{(1)} = \frac{1}{T_3} \quad L_{12}^{(1)} = -\frac{R_4}{T_3} \quad (43)$$

$$L_{11}^{(2)} = \frac{N}{T_3 T_5 D_f^{(1)}} \quad L_{12}^{(2)} = -\frac{R_6 N + R_4 T_5 T_6 D_f^{(1)} D_b^{(1)}}{T_3 T_5 D_f^{(1)}}$$

where:

$$N = 1 - R_4 R_5 D_f^{(1)} D_b^{(1)}$$

$$D = (1 - R_4 R_5 D_f^{(1)} D_b^{(1)}) (1 - R_1 R_6 D_f^{(2)} D_b^{(2)}) - R_1 R_4 T_5 T_6 D_f^{(1)} D_f^{(2)} D_b^{(1)} D_b^{(2)} \quad (44)$$

From this, we see immediately that the threshold condition (42) is here $D = 0$, which means (after cancellation of the factors between square brackets in Appendix B):

$$(1 - R_4 R_5 e^{2\Gamma L^{(1)}}) (1 - R_1 R_6 e^{2\Gamma L^{(2)}}) - R_1 R_4 T_5 T_6 e^{2\Gamma(L^{(1)} + L^{(2)})} = 0 \quad (45)$$

And, using (40) and (41) with (43), we can now compute the emission spectrum.

As an example, let us take the same device as in section 7 (with anti-reflection coating), but with a phase shifter of length $\Lambda/2$ ($= 118.1$ nm) in the middle of the device. By solving (45), we find that the main mode is now at the Bragg wavelength 1.528 μm , with a threshold amplitude gain of 10.93 cm^{-1} . The two next modes are at 1.5258 μm and 1.5302 μm , with a threshold amplitude gain of 34.63 cm^{-1} . We see that the degeneracy of the lasing mode is lifted and we have a good control on the lasing frequency.

In Figure 6, we show the calculated spectrum for two values of the amplitude gain (5 and 10.5 cm^{-1}). Notice that the two peaks on either side of the main mode do not correspond to the next modes (we will discuss this in the next section). The other bumps in the spectrum do correspond to longitudinal modes. They are much closer to one another than to the central mode because the variation of the phase of the reflectivity of the periodic sections with wavelength is

much faster outside the stop-band.

10. Spontaneous emission in a periodic waveguide

In Figure 6 we notice something strange: the two peaks adjacent to the main mode do not increase but decrease with increasing gain! This is because they do not correspond to any mode that is below threshold as the other peaks in the spectrum do, but are due to the way the spontaneous emission couples to the periodic waveguide. Indeed, if we trace where these peaks come from, we see that they come from the following factor S in (35) and (41):

$$S = \frac{1}{|\Gamma + (\Gamma + j2K_B)s^2|^2} \quad (46)$$

and that factor arose in section 5, when we computed the coupling to the waveguide. Figure 7 shows S for the same device and two same values of the amplitude gain as in Figure 6.

To understand physically why this is happening, we must remember that cavities can influence spontaneous emission because they modify the spectral density of electromagnetic modes available [6]. Indeed, Fermi's Golden Rule:

$$W_{fi} = \frac{2\pi}{\hbar} |\langle f | H' | i \rangle|^2 \rho_f \quad (47)$$

says that the transition rate is proportional to ρ_f is the density of final states (H' is the interaction Hamiltonian). In this case, what we have is not really a change of the total spontaneous emission rate, but a modification of the spectral and spatial distribution of the modes and thus of the spontaneous photons (as in [9,10]). The mode distribution in the case of an infinite space periodic in one dimension was worked out in [6]. (And the radiation pattern of a dipole in such a space was calculated in [11].) It turns out that the spontaneous emission is enhanced at the edges of the stop-band and decreased in the stop-band. From (11) and [5], we can see that this means that these spontaneous emission peaks will be situated at:

$$\lambda_{peak} = \frac{2\pi n_{eff}}{K_B \pm \kappa} \quad (48)$$

This can also be seen from (46), since the denominator has to be close to zero for S to be large and that means s^2 close to one. From (11), we can see that this happens only at the edges of the

stop-band (i.e., $\delta = \pm \kappa$).

This prediction of the behavior of the spectrum of a $\lambda/4$ phase shifted DFB laser should be verified experimentally by measuring the evolution of the emission spectrum below threshold as the pump current is changed. In a normal DFB laser, this would be much more difficult to observe since the position of the modes is very close to these spontaneous emission peaks. Nevertheless, in Figure 3 and 4, we can see some small bumps due to these spontaneous emission peaks. The main feature that reveals their nature is the fact that they decrease with increasing gain, relatively to the other peaks.

Notice that if this can be observed in real devices, it would give us the first practical mean to measure directly the coupling coefficient κ in a DFB laser, by using (48).

If one wants to use the usual transmission matrix method (i.e., one matrix for each layer and each boundary [4]) to check the results obtained here for a layered medium, one should be very careful with how the coupling of the source with the structure is done. The naive approach of assuming that the source emits plane waves of the form $\exp(\pm j \beta z)$ is false because these plane waves do not satisfy the differential equation [such as (19)]. The correct way to do it is similar to what we did in (20)-(22): use the two linearly independent solutions of the differential equation (which are each a combination of plane waves) and express the continuity of the fields. Then the result can be again decomposed in plane waves for use in the transmission matrices.

11. DBR lasers

Up to now, we have considered only the case when the spontaneous emission takes place in a periodic region. But in DBR lasers, the active region is uniform and there is no spontaneous emission in the periodic regions that act as mirrors. Also, in multisection lasers, there are often uniform active regions. So, we should consider this case also.

Actually, all we have to do is take the result we got for the periodic case and eliminate the periodicity, i.e., take $\kappa = 0$. This gives us then $s = 0$ and $\Gamma = (g - j \beta) = (g - j n_{eff} k_0)$. We get then, instead of (41):

$$\gamma^{(i)}(\lambda) = \frac{\pi}{2 n^{(i)}} \frac{\Gamma_c^{(i)} K_p^{(i)}}{w_{eff}^{(i)} d^{(i)}} \frac{1}{|T_{11}|^2} \frac{1}{|g^{(i)} - j \beta^{(i)}|^2} \quad (49)$$

$$\times \frac{1}{2g^{(i)}L^{(i)}} \left[|L_{11}^{(i)}|^2 (1 - e^{-2g^{(i)}L^{(i)}}) + |L_{12}^{(i)}|^2 (e^{2g^{(i)}L^{(i)}} - 1) \right]$$

This is a slight approximation, since we neglect some interference terms. But they are of order $(g/\beta) \approx 10^{-3}$ compared to the terms in (49).

If we have a simple DBR laser, this is the only contribution to the spectrum. If the uniform section is a part of a more complicated structure, we can then use this in (40). Actually, this formula is also valid for a Fabry-Perot laser, if we use the correct transmission matrix elements.

As an example of DBR laser, let us take a typical surface-emitting structure such as the one shown in Figure 8 (similar to the one in [12]). It is a AlGaAs/GaAs device with a GaAs active region that has a length $L_p = 2 \mu\text{m}$ ($n = 3.620$). The top and bottom mirrors have 25 and 42 pairs of layers, respectively. Each pair consists of a $Al_{0.05}Ga_{0.95}As$ layer ($n = 3.565$, 61.7 nm thick) and a $Al_{0.45}Ga_{0.55}As$ layer ($n = 3.292$, 66.8 nm thick). The substrate is also GaAs ($n = 3.620$). All refractive indices are at the center wavelength of 880 nm (these were computed using a model developed in [6]). A correct complete solution would involve taking into account the change of refractive index with wavelength and the losses in the mirrors (this was done in [6]), but here, for simplicity, we will neglect the losses and assume a constant refractive index. By computing the first Fourier coefficients, we find that $n_{eff} = 3.4231$ and $\kappa = 6192.5 \text{ cm}^{-1}$.

Again, the location of the origin and the boundaries is important because the dielectric reflections at the ends of the mirrors will be in phase or out of phase with the Bragg reflections depending on the phase of the grating. In Figure 8, we take $z_1 = 30.85 \text{ nm}$ and $z_2 = -3181.65 \text{ nm}$ (but any translation by a multiple of $\Lambda = 128.5 \text{ nm}$ is also good). And we also take $z'_1 = 30.85 \text{ nm}$ and $z'_2 = -5366.15 \text{ nm}$. This gives us $L_1 = 5.397 \mu\text{m}$ for the bottom mirror and $L_2 = 3.2125 \mu\text{m}$ for the top mirror. The reflection and transmission coefficients in Figure 8 are for the whole mirrors and are given in Appendix C.

The matrix elements we need are:

$$\frac{L_{11}}{T_{11}} = \frac{T'_1}{D'} \quad \frac{L_{12}}{T_{11}} = -\frac{T'_1 R'_4 P_p^2}{D'} \quad (50)$$

where:

$$D' = 1 - R'_1 R'_4 P_p^2$$

$$P_p = \exp\left[(g_p - j\beta_p)L_p\right] \quad (51)$$

where g_p and β_p are the gain and propagation constant in the active region. The threshold condition is $D' = 0$, which means:

$$R'_1 R'_4 \exp\left[2(g_p - j\beta_p)L_p\right] = 1 \quad (52)$$

Notice that this is nearly identical to a Fabry-Perot threshold condition. The only difference is that here, the reflection coefficients have a phase that depends on wavelength.

With an active region length of 2 μm , we find that the main mode is at 878.22 nm with a threshold (amplitude) gain of 95.95 cm^{-1} . The next modes are at 854.34 nm (847 cm^{-1}) and 905.59 nm (535.9 cm^{-1}). They are not placed symmetrically with respect to the main mode because the mirrors are not symmetrical, due to their different thicknesses and the presence of the dielectric reflection at the air interface on top.

Because of the large difference in threshold gains, we see that this device should be single longitudinal mode. A rough estimate of the threshold current can be made, assuming a device 10 μm in diameter. The carrier density for obtaining an intensity gain of 190 cm^{-1} at 878 nm can be estimated at about $1.3 \times 10^{18} \text{ cm}^{-3}$ (using a model of the gain described in Appendix A of [6], for a n-type active region doped to 10^{18} cm^{-3}). If we assume a carrier lifetime of 4 ns, this gives us a threshold current of 8.2 mA, which is a reasonable number.

In Figure 9, we have plotted the calculated spectrum for this DBR surface-emitting laser for two values of the amplitude gain (10 and 95 cm^{-1}). This calculation assumed that the gain was the same at all wavelengths, which is not the case in practice. But it gives nevertheless a good idea of what the spectrum is going to look like. One spectrum was shifted downwards because the two spectra were nearly exactly on top of each other, except for the main mode (this is because we did not include an increase of the spontaneous emission as the gain increases). There is no spontaneous emission peaks in this case since the emission takes place in a uniform waveguide, not in a periodic one. The large separation between the main modes and the side modes is due to the large coupling coefficient κ of the mirrors in this case. Notice that the main mode position depends quite critically on the active region length L_p [as can be seen from (51)]. This effect and the effect of layer thickness variations were studied in detail in [13].

12. Conclusion

In this paper, we developed a general method for calculating the emission spectrum of lasers (mainly semiconductor lasers), using transmission matrices. We showed how that method could be applied to usual Fabry-Perot lasers and normal DFB lasers. Then, we developed a general formalism for multi-section DFB lasers and applied it to a DFB laser with a $\lambda/4$ phase shifter. In doing that, we discovered some interesting features of the spontaneous emission in a periodic waveguide that should be investigated further. If confirmed by experiment, this would give for the first time a direct way to measure the coupling coefficient κ in a DFB laser. The previous work by Soda and Imai [1] did not show this characteristic probably because of their incorrect treatment of the coupling of the source to the modes and the neglect of interference terms in their calculations.

Next, we showed how to extend the results to structures with uniform sections and to DBR lasers. As an example, we calculated the emission spectrum of a surface-emitting DBR laser. We pointed out that the major differences between DBR and Fabry-Perot lasers are due mainly to the wavelength dependence of the phase of the reflections for DBR mirrors.

Acknowledgments

This work was supported by the Air Force Rome Air Development Center (US Gov. contract F19628-89-C-0177) and Lockheed Missiles and Space Company (Subcontract SF070A0170R).

Appendix A

The reflection and transmission coefficients in Figure 2 are:

$$\begin{aligned}
 R_1 &= \frac{r - s_{f1}}{1 - r s_{b1}} \left[\frac{1 + s_{b1}}{1 + s_{f1}} \right] & R_2 &= \frac{s_{b1} - r}{1 - r s_{b1}} \\
 T_1 &= (1 + r) \frac{1 - s_{f1} s_{b1}}{(1 - r s_{b1})} \left[\frac{1}{1 + s_{f1}} \right] & T_2 &= \frac{1 - r}{1 - r s_{b1}} \left[1 + s_{b1} \right]
 \end{aligned} \tag{A.1}$$

and

$$\begin{aligned}
 R_3 &= \frac{s_{f2} - r}{1 - r s_{f2}} & R_4 &= \frac{r - s_{b2}}{1 - r s_{f2}} \left[\frac{1 + s_{f2}}{1 + s_{b2}} \right] \\
 T_3 &= \frac{1 - r}{1 - r s_{f2}} \left[1 + s_{f2} \right] & T_4 &= (1 + r) \frac{1 - s_{b2} s_{f2}}{1 - r s_{f2}} \left[\frac{1}{1 + s_{b2}} \right]
 \end{aligned} \tag{A.2}$$

where r is the reflection coefficient due to the change in propagation constant (between the guide and air in this case):

$$r = \frac{K_B - k_0}{K_B + k_0} = \frac{n_{eff} - 1}{n_{eff} + 1} \tag{A.3}$$

The factors inside square brackets always cancel each other when combined in formulas and can be omitted.

Appendix B

In Figure 5, R_i and T_i are the same as in Appendix A for $i = 1,2,3,4$, except that z_1 (for $i = 1,2$) is replaced by $z_1^{(2)}$ and z_2 (for $i = 3,4$) is replaced by $z_2^{(1)}$. The reflection and transmission coefficients for the phase shifter are given by:

$$\begin{aligned} R_5 &= \frac{P_p^2 s_{f2} - s_{f1}}{1 - P_p^2 s_{b1} s_{f2}} \left[\frac{1 + s_{b1}}{1 + s_{f1}} \right] & T_5 &= \frac{P_p (1 - s_{f1} s_{b1})}{1 - P_p^2 s_{b1} s_{f2}} \left[\frac{1 + s_{f2}}{1 + s_{f1}} \right] \\ R_6 &= \frac{P_p^2 s_{b1} - s_{b2}}{1 - P_p^2 s_{b1} s_{f2}} \left[\frac{1 + s_{f2}}{1 + s_{b2}} \right] & T_6 &= \frac{P_p (1 - s_{f2} s_{b2})}{1 - P_p^2 s_{b1} s_{f2}} \left[\frac{1 + s_{b1}}{1 + s_{b2}} \right] \end{aligned} \quad (\text{B.1})$$

where the subscript 1 means $z_1^{(1)}$ and 2 means $z_2^{(2)}$ (both are zero in this case, so we have actually $s_{f1} = s_{b1} = s_{f2} = s_{b2} = s$). And P_p is the propagation factor in the phase-shifter:

$$P_p = \exp \left[(g - j\beta_p) L_p \right] \quad (\text{B.2})$$

where g and β_p are the gain and propagation constant, respectively. The formulas (B.1) can easily be established by using the formulas of Appendix A (with $r = 0$) and the method of multiple reflection [6]. Again, the factors inside square brackets will cancel and can be omitted.

Appendix C

For the spectrum and threshold calculation of the DBR of Figure 8, we need only three coefficients. The first two are:

$$R'_1 = R_3 + \frac{T_3 T_4 R_1 D_f^{(2)} D_b^{(2)}}{1 - R_1 R_4 D_f^{(2)} D_b^{(2)}} \quad (C.1)$$

$$T'_1 = \frac{T_1 T_3 D_f^{(2)}}{1 - R_1 R_4 D_f^{(2)} D_b^{(2)}}$$

where R_1, T_1 are the same as in Appendix A and R_3, R_4, T_3, T_4 are also the same, except that r is replaced by r_a given by:

$$r_a = \frac{n_{eff} - n_a}{n_{eff} + n_a} \quad (C.2)$$

where n_a is the refractive index of the active region. Again, the factors inside square brackets cancel out.

The third coefficient we need is:

$$R'_4 = R_2 + \frac{T_1 T_2 R_4 D_f^{(1)} D_b^{(1)}}{1 - R_1 R_4 D_f^{(1)} D_b^{(1)}} \quad (C.3)$$

where R_4 is the same as in Appendix A, but with z'_2 replacing z_2 and R_1, R_2, T_1, T_2 are also the same, except for r replaced by r_a and z_2 replaced by z'_2 . Once more, the factors between square brackets cancel out.

REFERENCES

- [1] H. Soda and H. Imai, "*Analysis of the Spectrum Behavior Below the Threshold in DFB Lasers*", IEEE J. Quantum Elec., QE-22 (5), pp 637-641, 1986.
- [2] S. Wang, "*Thin-film Bragg lasers for integrated optics*", Wave Electronics, vol 1, pp 31-59, 1974-1975.
- [3] A. Yariv and A. Grover, "*Equivalence of the coupled-mode and Floquet-Bloch formalism in periodic optical waveguides*", Appl. Phys. Lett., vol 26, pp 537-539, 1975.
- [4] A. Yariv and P. Yeh, "*Optical waves in crystals*", Wiley, New York, 1984, see Chapter 6.
- [5] S. Wang, in: *Semicond. and Semimetals*, Vol 22, Part E (W.T. Tsang editor), see pp 52-64 (1985).
- [6] J.-P. Weber, "*Propagation of Light in Periodic Structures: Application to the Surface-Emitting Laser-Diode*", Ph.D. dissertation, Electrical Engineering and Computer Sciences, UC Berkeley, June 1990.
- [7] K. Petermann, "*Calculated spontaneous emission factor for double-heterostructure injection lasers with gain-induced waveguiding*", IEEE J. Quantum Electron., QE-15 (7), pp 566-570, July 1979.
- [8] Any book on electromagnetism which use rationalized MKSA units, such as: S. Ramo, J.R. Whinnery, and T. Van Duzer, "*Fields and waves in communication electronics*", (2nd edition), Wiley, New York, 1984.
- [9] E. Yablonovitch, "*Inhibited spontaneous emission in solid-state physics and electronics*", Phys. Rev. Lett., 58 (20), pp 2059-2062, 18 May 1987.
- [10] E. Yablonovitch, T.J. Gmitter, and R. Bhat, "*Inhibited and enhanced spontaneous emission from optically thin AlGaAs/GaAs double heterostructures*", Phys. Rev. Lett., 61 (22), pp 2546-2549, 28 November 1988.
- [11] K.F. Casey, "*Dipole radiation in a periodically stratified medium*", Canad. J. of Physics, 46, pp 2543-2551, 1968.
- [12] W. Hsin, G. Du, J.K. Gamelin, K.J. Malloy, S. Wang, J.R. Whinnery, Y.J. Yang, T.G. Dziura, and S.C. Wang, "*Low threshold distributed Bragg reflector surface emitting laser diode*

with semiconductor air-bridge-supported top mirror'', Electron. Lett., 26 (5), pp 307-308, 1 March 1990.

- [13] J.-P. Weber, K. Malloy, and S. Wang, "*Effects of layer thickness variations on vertical-cavity surface-emitting DBR semiconductor lasers*", IEEE Photon. Technol. Lett., vol. 2, no. 3, pp 162-164, March 1990.

Figure Captions

Fig. 1 : Model for the transmission matrices.

Fig. 2 : Model of the Fabry-Perot cavity and definition of the reflection and transmission coefficients.

Fig. 3 : Emission spectrum of a DFB laser with anti-reflection coating, center wavelength in $1.528 \mu\text{m}$, $n_{\text{eff}} = 3.2336$, $\kappa = 100 \text{ cm}^{-1}$, $L = 300 \mu\text{m}$ for three different gains. Threshold gain (amplitude) is 20.754 cm^{-1} .

Fig. 4 : Emission spectrum of the same device as in Fig. 3, but without anti-reflection coating. (a) $z_2 = 0$, threshold gain (amplitude) = 10.635 cm^{-1} . (b) $z_2 = 100 \text{ nm}$, threshold gain (amplitude) = 8.896 cm^{-1} .

Fig. 5 : Model for the DFB laser with a $\lambda/4$ phase shifter in the middle. This figure defines the reflection and transmission coefficients.

Fig. 6 : Emission spectrum of a DFB laser with a $\lambda/4$ phase shifter. The device is the same as in Fig. 3, except for the phase shifter. Threshold gain (amplitude) is 10.927 cm^{-1} .

Fig. 7 : S factor of equation (46), for the device of Fig. 6. This is the factor giving the spontaneous emission peaks.

Fig. 8 : Model for a vertical-cavity surface-emitting DBR laser.

Fig. 9 : Emission spectrum for the device of Fig. 8. Center wavelength is 880 nm , $\kappa = 6192.5 \text{ cm}^{-1}$ and the active region is $2 \mu\text{m}$. The main mode is at 878.2 nm , with a threshold gain (amplitude) = 95.95 cm^{-1} . The two curves were shifted vertically to distinguish them better.

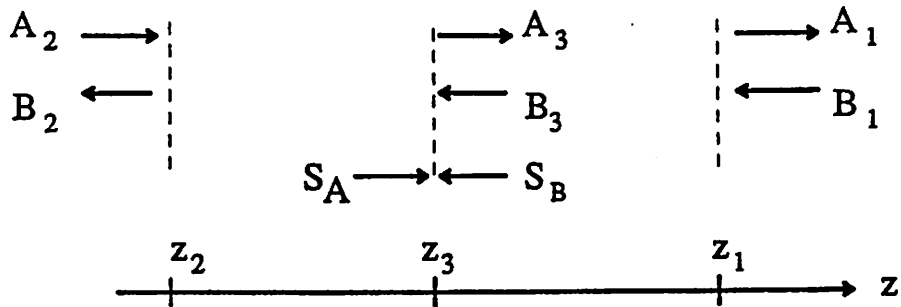


FIGURE 1

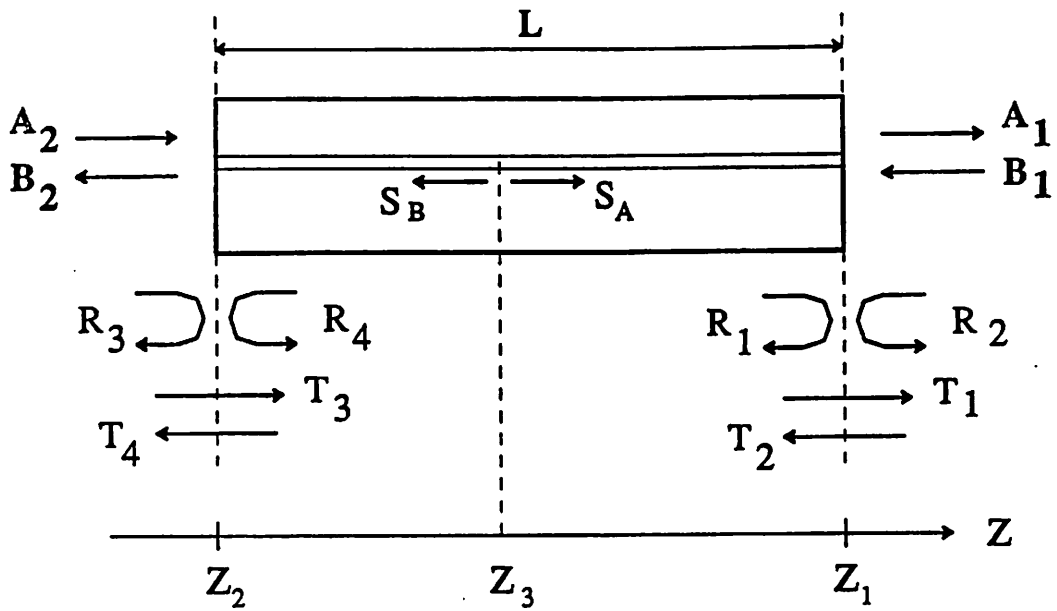


FIGURE 2

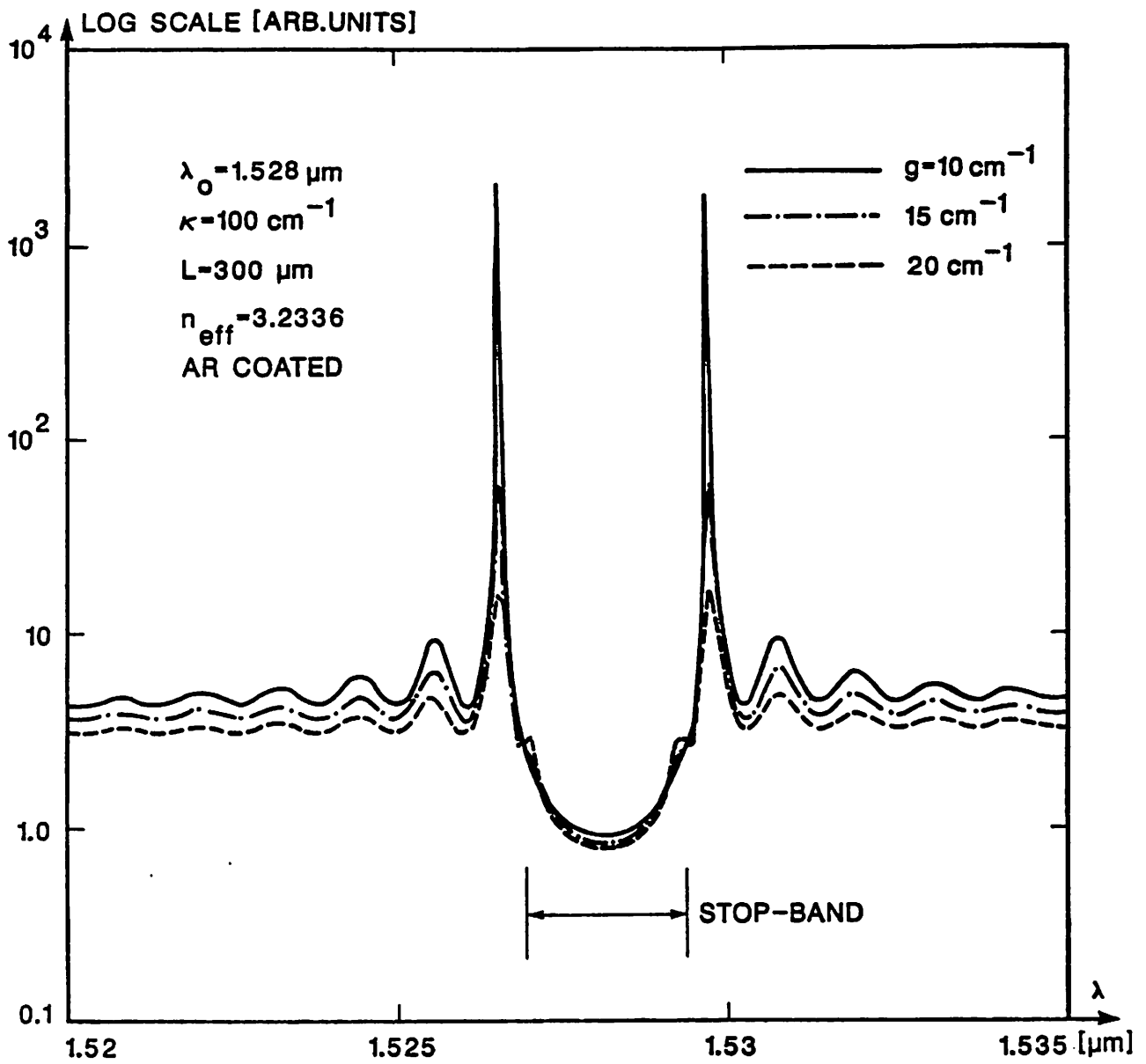


FIGURE 3

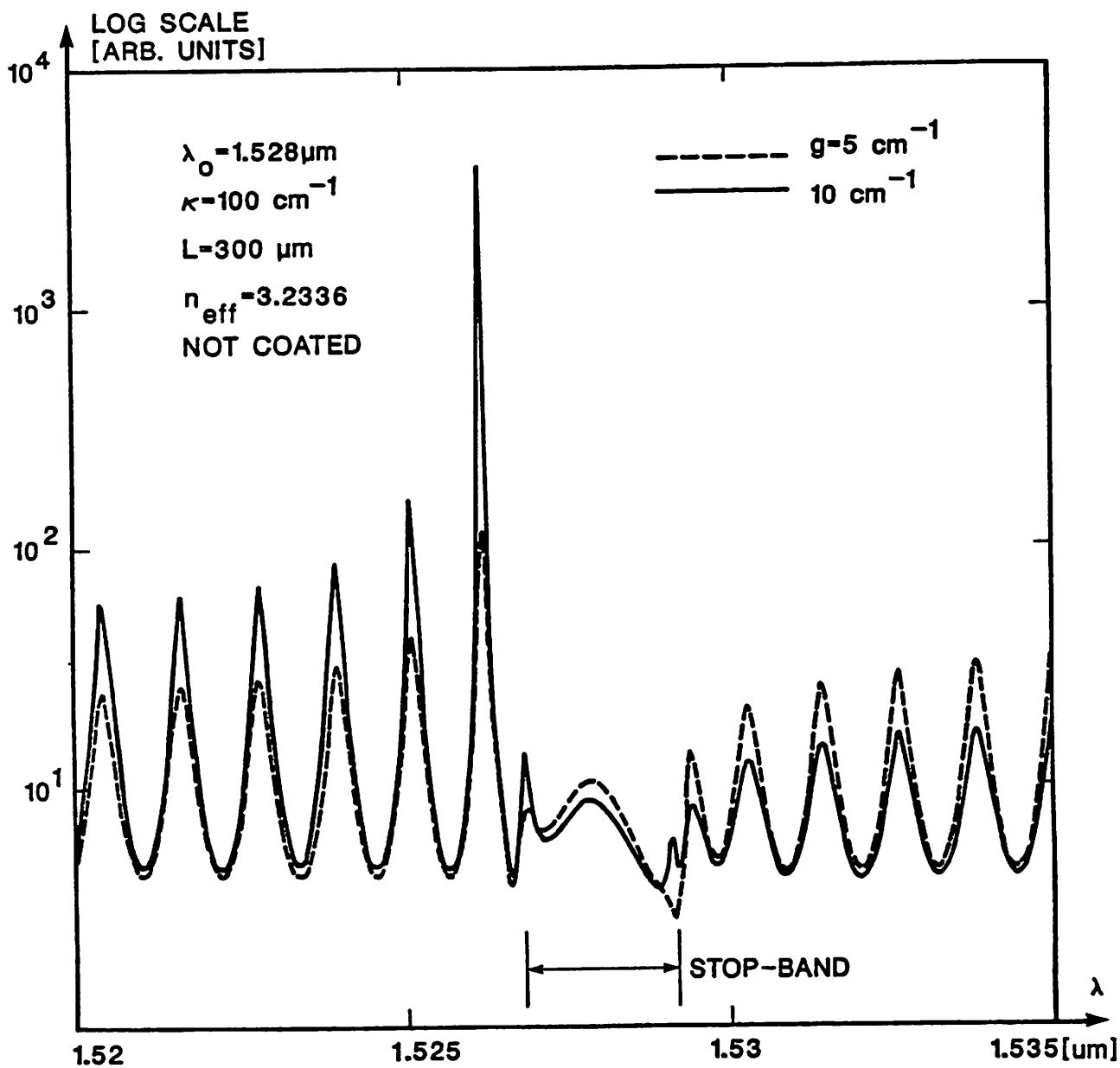


FIGURE 4 (2)

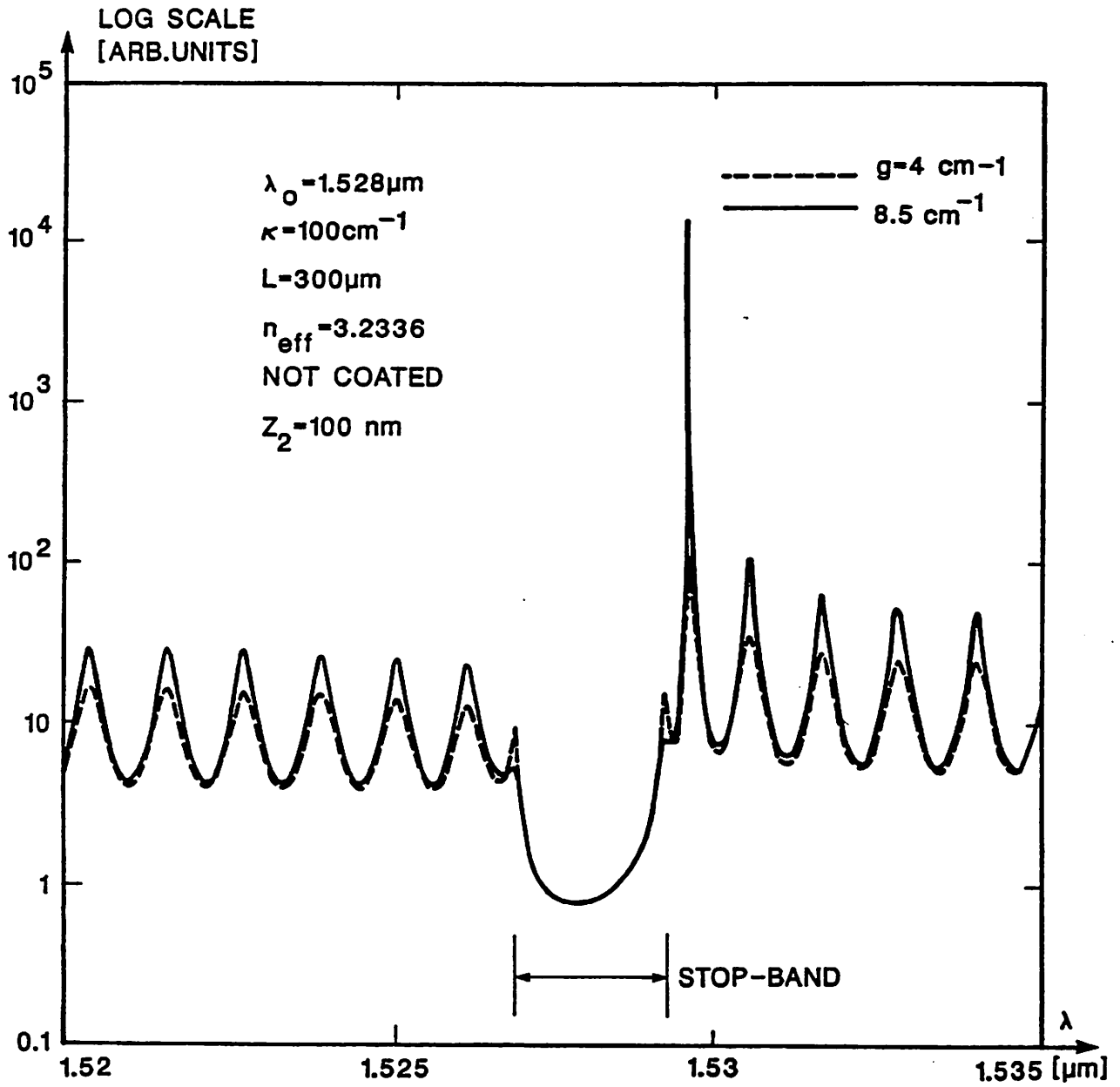


FIGURE 4 (b)

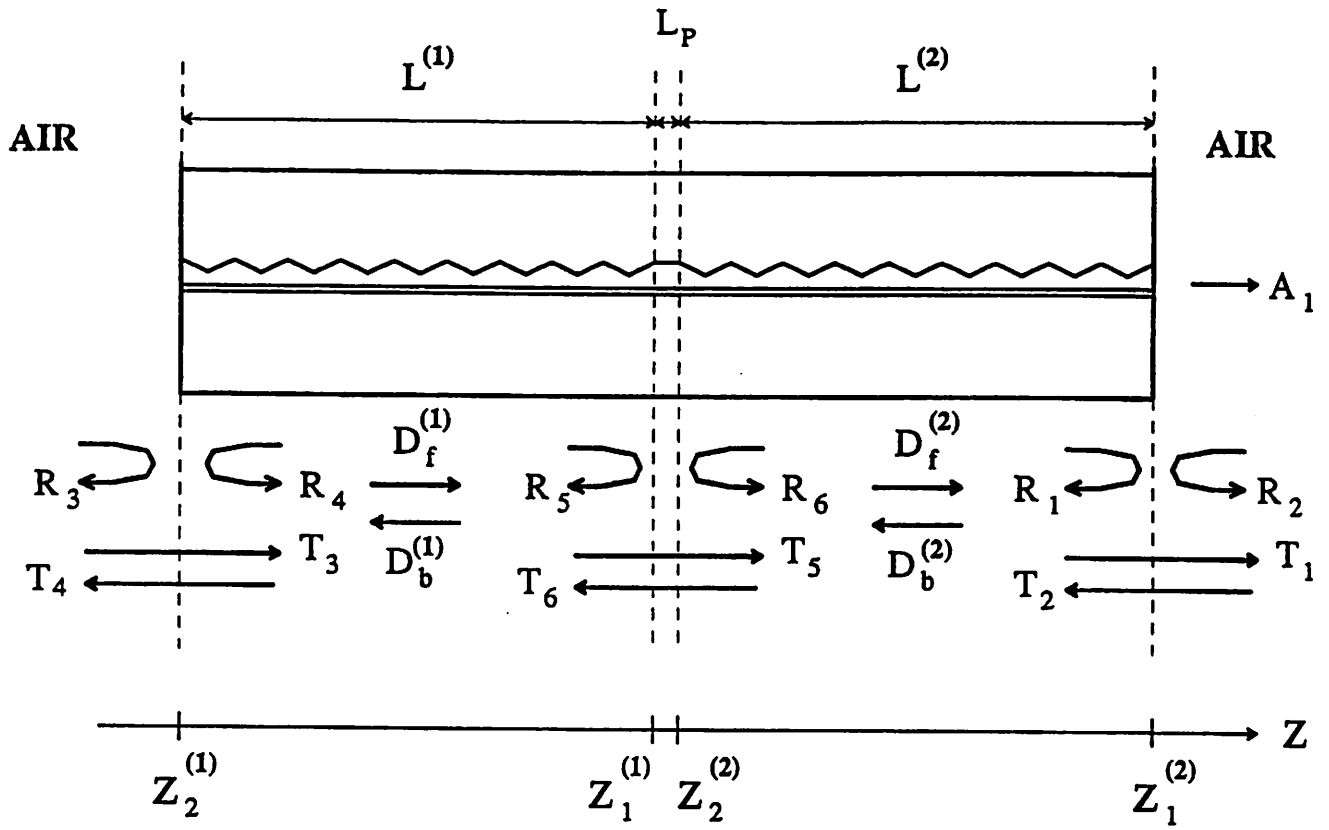


FIGURE 5

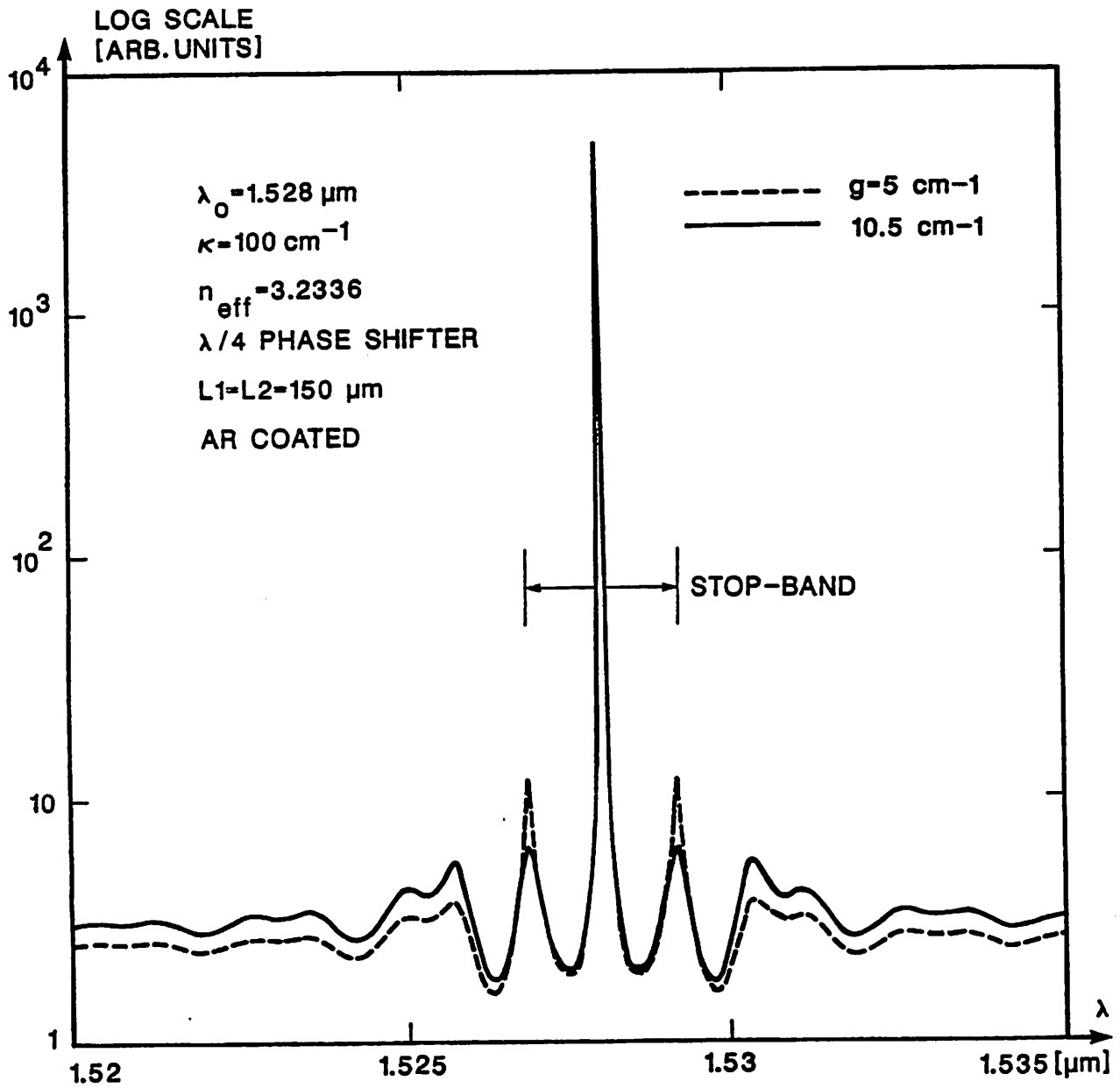


FIGURE 6

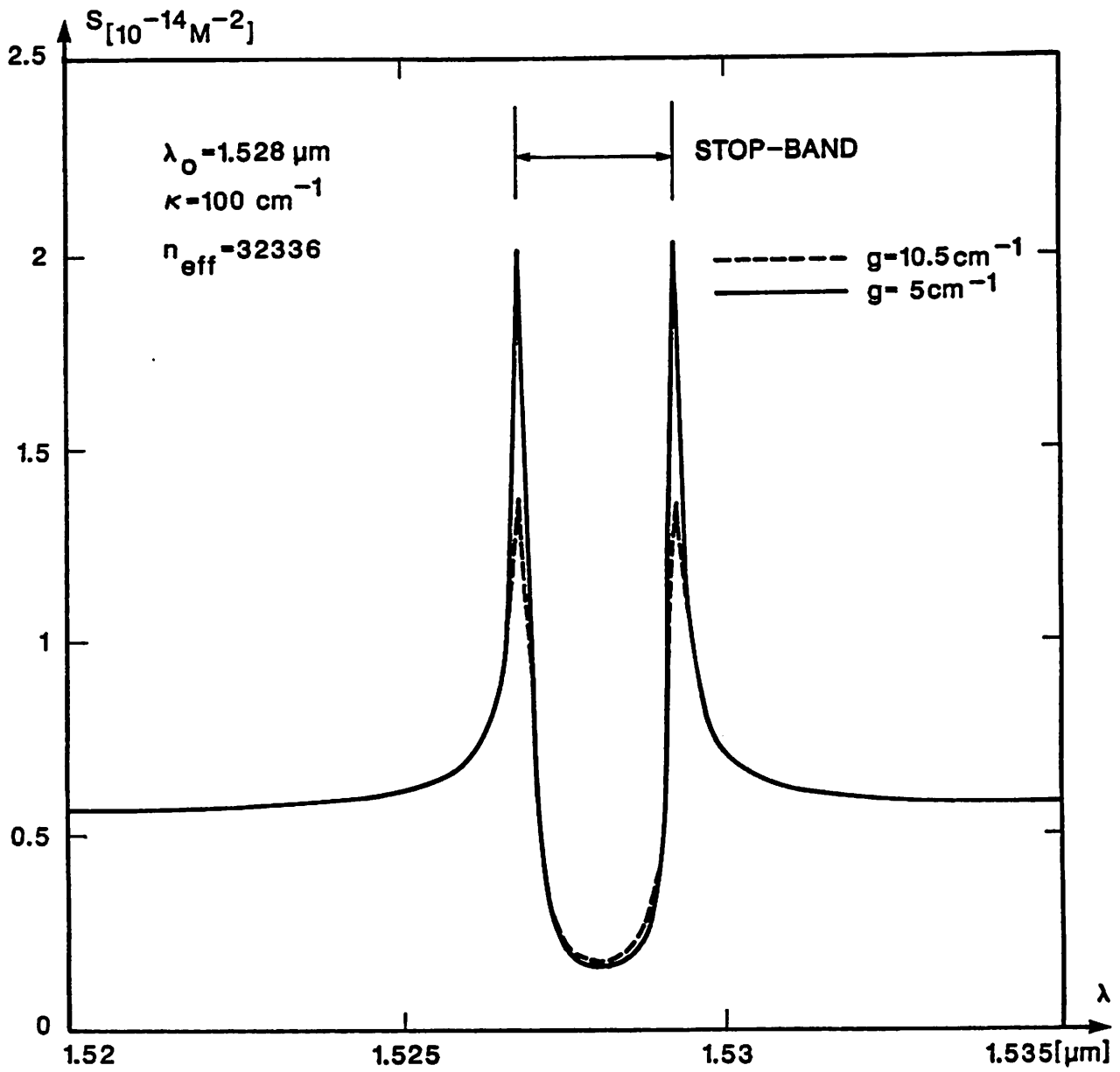


FIGURE 7

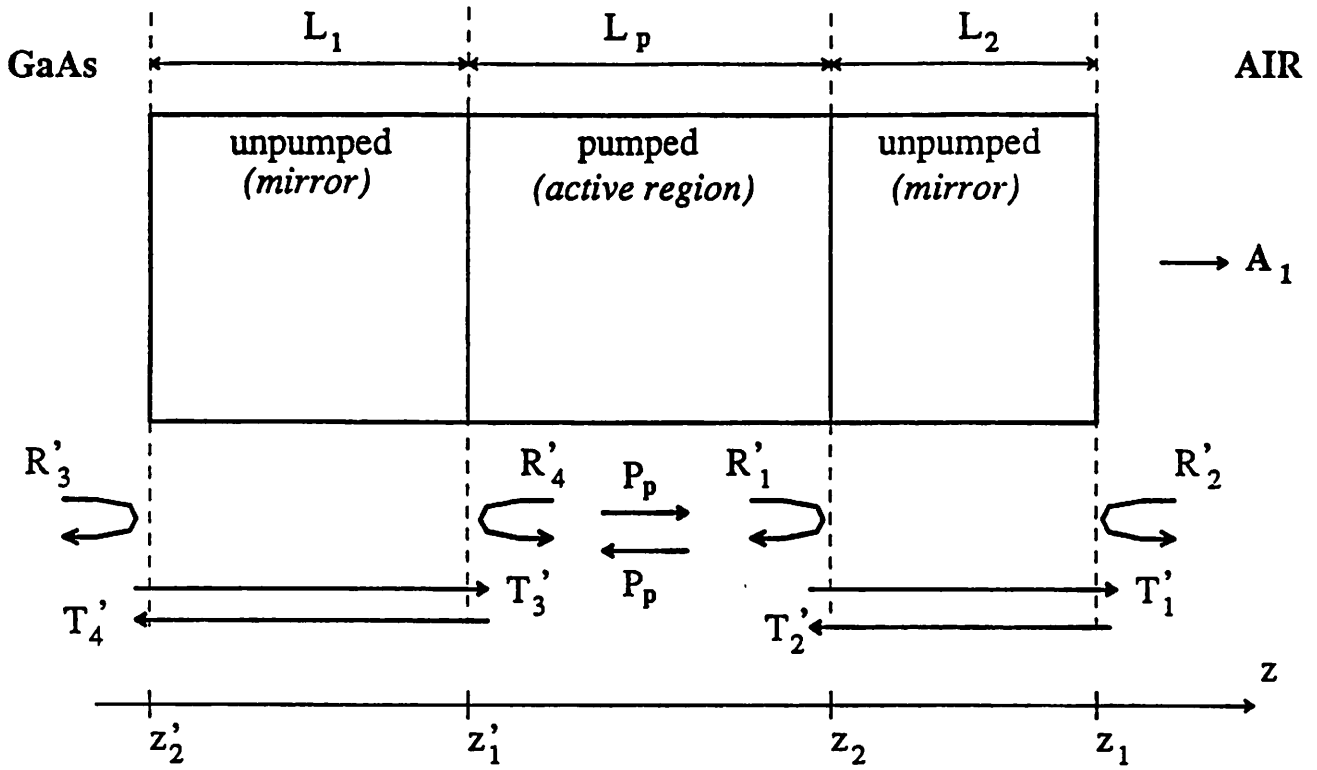


FIGURE 8

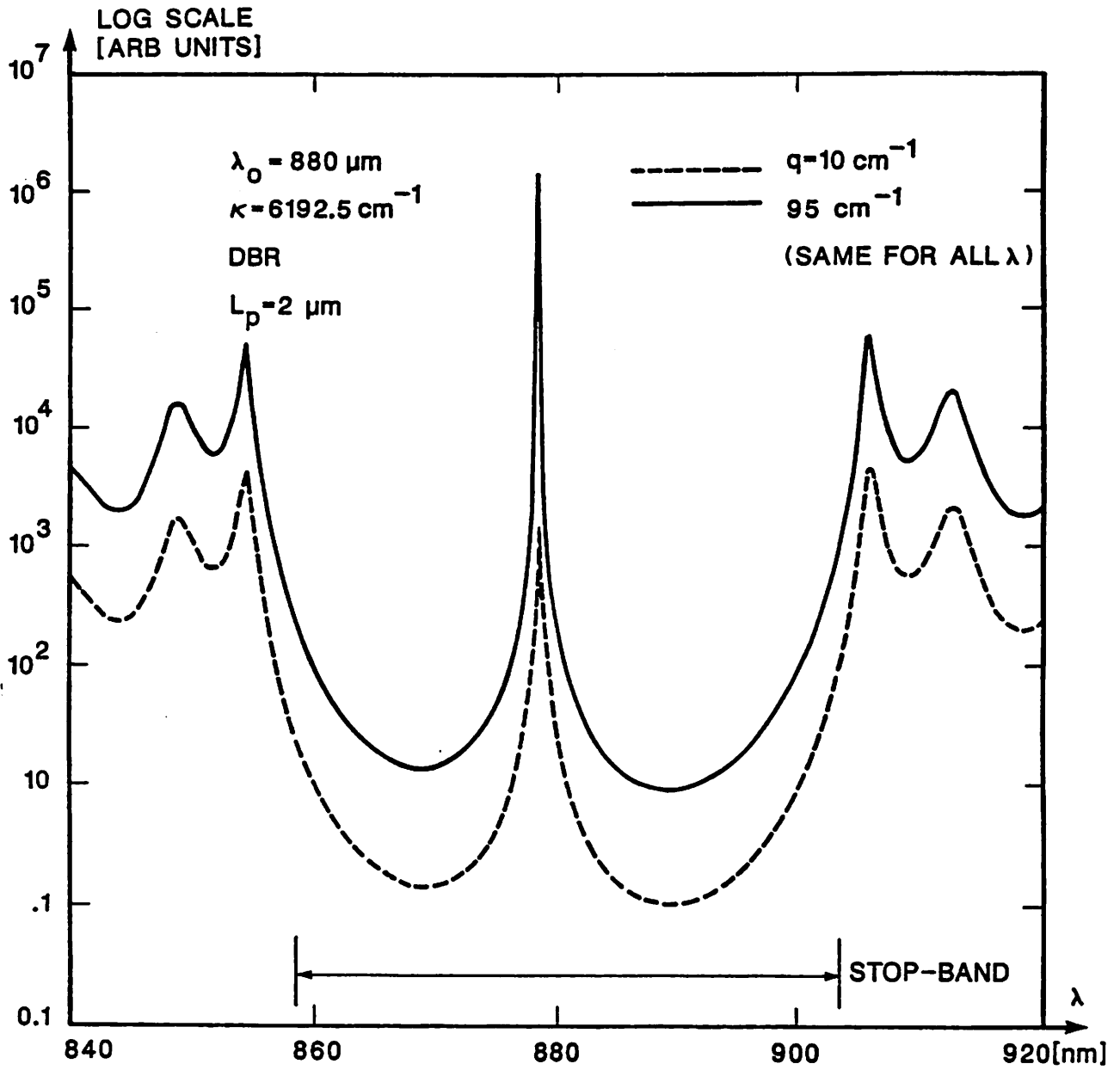


FIGURE 3